Targeted disruption of the three Rb-related genes leads to loss of G_1 control and immortalization

Julien Sage,[1] George J. Mulligan,[1,3] Laura D. Attardi,[1,4] Abigail Miller,[1] SiQi Chen,[1] Bart Williams,[1] Elias Theodorou,[1] and Tyler Jacks[1,2,5]

[1]Department of Biology and Center for Cancer Research, [2]Howard Hughes Medical Institute, Massachusetts Institute of Technology, Cambridge, Massachusetts 02139, USA

The retinoblastoma protein, pRB, and the closely related proteins p107 and p130 are important regulators of the mammalian cell cycle. Biochemical and genetic studies have demonstrated overlapping as well as distinct functions for the three proteins in cell cycle control and mouse development. However, the role of the pRB family as a whole in the regulation of cell proliferation, cell death, or cell differentiation is not known. We generated embryonic stem (ES) cells and other cell types mutant for all three genes. Triple knock-out mouse embryonic fibroblasts (TKO MEFs) had a shorter cell cycle than wild-type, single, or double knock-out control cells. TKO cells were resistant to G_1 arrest following DNA damage, despite retaining functional p53 activity. They were also insensitive to G_1 arrest signals following contact inhibition or serum starvation. Finally, TKO MEFs did not undergo senescence in culture and do possess some characteristics of transformed cells. Our results confirm the essential role of the Rb family in the control of the G_1/S transition, place the three Rb family members downstream of multiple cell cycle control pathways, and further the link between loss of cell cycle control and tumorigenesis.

[*Key Words*: *Rb*; MEFs; knock-out; G_1 control; immortalization]

Received August 14, 2000; revised version accepted October 24, 2000.

The *RB* tumor suppressor gene has been implicated in a wide variety of human tumors, including familial retinoblastomas and osteosarcomas, as well as sporadic lung, prostate, bladder, and breast carcinomas (Goodrich and Lee 1993). The pRB protein is thought to be a critical component in the control of the restriction point of the G_1/S transition of the cell cycle (Weinberg 1995). pRB inhibits the expression of genes required for S-phase entry and progression by directly binding to the E2F family of transcriptional factors, resulting in transcriptional inhibition and active repression of these genes (Dyson 1998). Near the G_1/S transition, pRB is sequentially phosphorylated by cyclin D-CDK4,6 and cyclin E-CDK2 complexes, leading to release of E2F from pRB, activation of E2F target genes and S-phase entry (Weinberg 1995; Dyson 1998). The assembly and activity of the cyclin-CDK complexes are regulated by the cyclin kinase inhibitors of the INK4 and CIP/KIP families (Hengst and Reed 1998; Ruas and Peters 1998).

Present addresses: [3]Millenium Predictive Medicine, Cambridge, MA 02139, USA; [4]Stanford University School of Medicine, Department of Radiation Oncology, Stanford, CA 94305, USA.
[5]Corresponding author.
E-MAIL tjacks@mit.edu; FAX (617) 253-9863.
Article and publication are at www.genesdev.org/cgi/doi/10.1101/gad.843200.

This simple scheme is complicated by the existence of two genes structurally and functionally related to *RB*, *p107*, and *p130* (Mulligan and Jacks 1998). The three proteins of the pRB family have similar properties, such as binding to E2F family members (Dyson 1998). Each pRB family member is also able to inhibit cell cycle progression when ectopically expressed (Harbour and Dean 2000). However, there is growing evidence that the three pRB family members also have distinct cellular and developmental functions. They are differentially expressed during mouse development (Jiang et al. 1997), and their ability to arrest the cell cycle can be cell-type specific (Zhu et al. 1993). In addition, the different pRB family members preferentially associate with different E2F family members during cell cycle progression, and functional differences may exist between these complexes (Dyson 1998).

To begin to define the individual roles of pRB related proteins in vivo, the three genes have each been inactivated in mice. $Rb^{-/-}$ embryos die at midgestation with inefficient erythropoiesis, as well as abnormal cell cycle entry and cell death in the liver, lens, and nervous system (Clarke et al. 1992; Jacks et al. 1992; Lee et al. 1992). These defects can be partially or completely ameliorated through combined mutation of *E2f-1*, suggesting that increased E2F activity is responsible for many of the effects

of *Rb* deficiency in embryogenesis (Tsai et al. 1998). $Rb^{+/-}$ mice and chimeric animals made with $Rb^{-/-}$ ES cells develop pituitary and thyroid tumors but not retinoblastoma or any of the tumors commonly associated with *RB* mutation in humans (Clarke et al. 1992; Jacks et al. 1992; Lee et al. 1992; Maandag et al. 1994; Williams et al. 1994). In contrast, $p130^{-/-}$ and $p107^{-/-}$ mice do not have any obvious developmental or tumor phenotype on 129/Sv or C57BL/6 genetic backgrounds (Cobrinik et al. 1992; Lee et al. 1996). Interestingly, on a Balb/c genetic background, *p107* and *p130* mutations do have phenotypic effects (LeCouter et al. 1998a,b). Also, there are some examples of functional inactivation of *p107* or *p130* in human tumors (Takimoto et al. 1998; Claudio et al. 2000), suggesting that in certain settings, *p107* and *p130* may have an essential role in cell cycle control.

Analysis of double-mutant mice has also provided evidence for overlapping roles of the three family members in mouse development and cell cycle control. $Rb^{-/-}$; $p107^{-/-}$ and $Rb^{-/-}$;$p130^{-/-}$ embryos die earlier during mouse development than $Rb^{-/-}$ embryos, with more pronounced cell cycle defects and increased cell death (Lee et al. 1996; G.J. Mulligan and T. Jacks, unpubl.). On a mixed 129/SvxC57BL/6 genetic background, $p130^{-/-}$; $p107^{-/-}$ mice die just after birth with defects in bone formation and abnormalities in chondrocyte proliferation (Cobrinik et al. 1996). Studies using single- or double-mutant T lymphocytes have shown that p107 can effectively compensate for absence of p130 in this cell type, and that the levels of pRB:E2F complexes increase in $p130^{-/-}$;$p107^{-/-}$ T cells (Mulligan et al. 1998). Finally, chimeric mice produced by injection of $Rb^{-/-}$; $p107^{-/-}$ ES cells developed retinoblastomas (Robanus-Maandag et al. 1998), demonstrating that in the context of *Rb* deficiency, *p107* can act as a tumor suppressor gene in mice.

The effect of Rb family mutations has also been examined in mouse embryonic fibroblasts (MEFs) in culture. $Rb^{-/-}$ and $p107^{-/-}$;$p130^{-/-}$ fibroblasts (Herrera et al. 1996; Hurford et al. 1997) each have mild defects in cell cycle regulation and show differences in the inappropriate expression of cell cycle–regulated genes. pRB, but not p107 or p130, is required for terminal differentiation and for maintenance of the postmitotic state of MEFs induced to differentiate in the myogenic lineage (Novitch et al. 1996).

The adenovirus E1A, SV40 Large T, and human papillomavirus E7 oncoproteins all bind to the three pRB family proteins (Zalvide and DeCaprio 1995; Flint and Shenk 1997; Smith-McCune et al. 1999) and have been extensively used to study the function of the *RB* family. Mutations that prevent binding to pRB, p107, and p130 also impair the ability of these viral proteins to transform cells, indicating that such interactions are necessary for viral transformation (Nevins 1994). While experiments using $Rb^{-/-}$ fibroblasts indicate that pRB may be the critical target for this interaction domain of adenovirus E1A in cellular transformation in this cell type (Samuelson and Lowe 1997), inactivation of other pRB-related proteins may be important in other cells. Also, experiments with viral oncoproteins have suggested a role for the *RB* family as a whole in the cellular response to DNA damage (Demers et al. 1994; Slebos et al. 1994). However, these viral oncoproteins interact with many other cellular proteins (Whyte et al. 1989) and also interact differently with each pRB family member (Smith-McCune et al. 1999), which complicates the interpretation of these experiments.

These results strongly indicate that the three *Rb* family members have shared as well as distinct roles in various cellular processes. However, because of this functional overlap, the exact role of the *Rb* family in controlling cell cycle is not fully understood. Also, the relative importance of each family member for processes as diverse as cell death, cell differentiation, or cell proliferation has not been addressed. To understand the role of the pRB family as a whole in various aspects of cell cycle control and to eliminate the possibility for functional compensation among the family members, we have generated cells genetically deficient for pRB, p107, and p130. Analysis of these triple knock-out cells in comparison with wild-type, single-, and double-mutant cells demonstrates a fundamental role of the *Rb* family in the control of the G_1/S transition and also highlights the functional overlap between the three family members in multiple aspects of cell cycle regulation.

Results

$p130^{-/-}$;$p107^{-/-}$;$Rb^{-/-}$ *TKO MEFs are viable and proliferate in culture*

To understand the functional similarities and differences between the three Rb family members, we wished to examine triple-mutant cells in culture in comparison with single- and double-mutant controls. Because of the previous analysis of $p107^{-/-}$;$p130^{-/-}$ and $Rb^{-/-}$ mouse embryonic fibroblasts (MEFs; Herrera et al. 1996; Hurford et al. 1997; Samuelson and Lowe 1997; Brugarolas et al. 1998; Harrington et al. 1998), we chose to generate and characterize triple knock-out (TKO) MEFs. To this end, $p107^{-/-}$;$p130^{-/-}$ embryonic stem (ES) cell lines were generated de novo from embryos obtained by breeding. One of these ES cell lines was shown to produce highly chimeric embryos and adult animals (data not shown) and was used to create TKO ES cells by two successive rounds of targeted homologous recombination into the *Rb* locus. Targeting of the first *Rb* allele was performed using a vector carrying the hygromycin resistance gene (Williams et al. 1994). Three $p107^{-/-}$;$p130^{-/-}$;$Rb^{+/-}$ subclones were isolated, and the second *Rb* allele was targeted in each of these subclones (Fig. 1A). The second *Rb* targeting vector carried a puromycin resistance gene and created a conditional allele of *Rb*, with two *lox*P sites surrounding exon 3. This strategy was employed to allow better control of the final targeting event in case cells lacking *Rb* family function were nonviable. After expression of the Cre recombinase, ES cell clones were tested by PCR and Southern blot for loss of *Rb* exon 3 (Figure 1A,B; data not shown). This deletion creates a frameshift

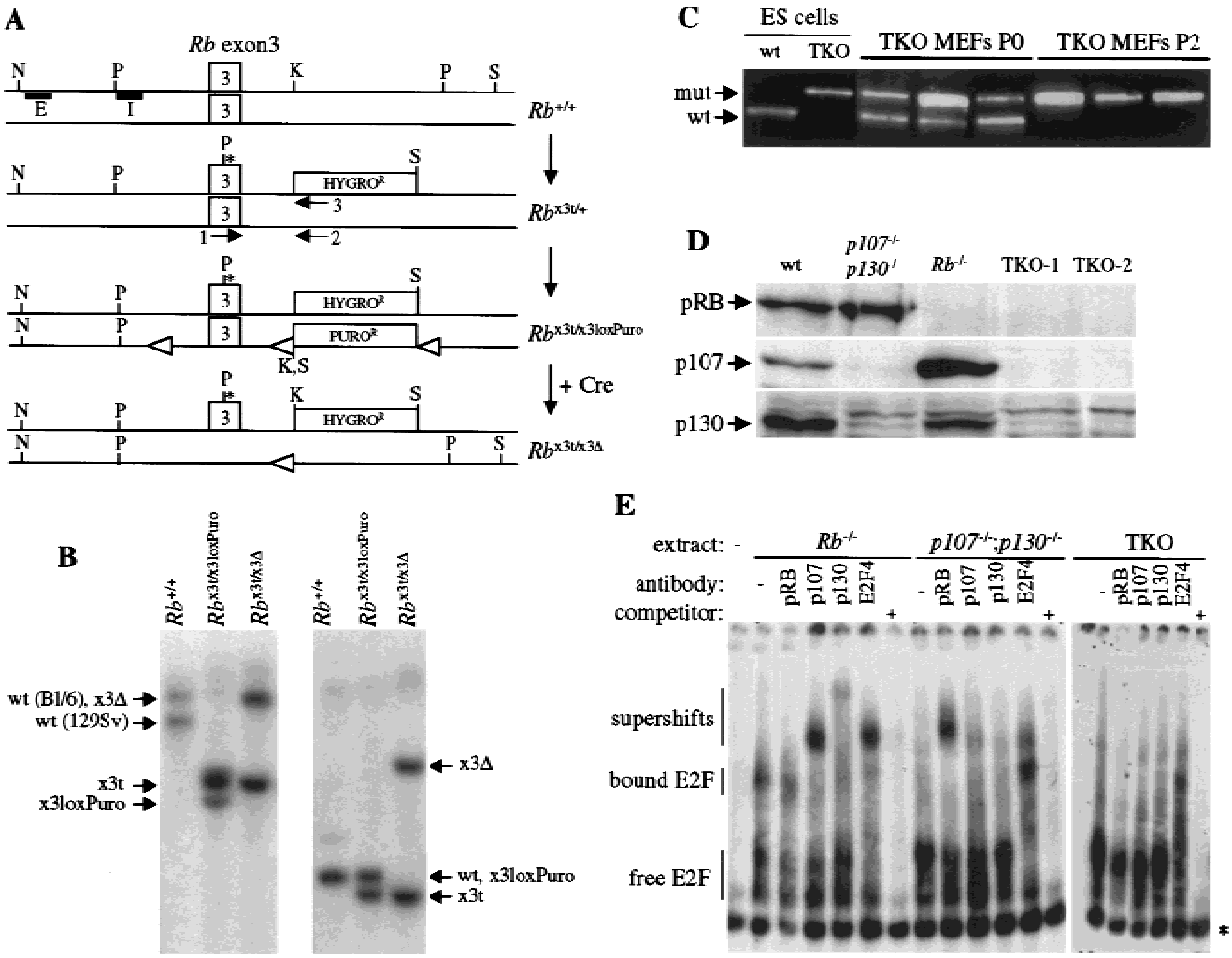

Figure 1. Creation of TKO ES cells and MEFs. (*A*) Targeting of the first *Rb* allele in $p107^{-/-};p130^{-/-}$ ES cells inserted a stop codon (*) in *Rb* exon 3 and a hygro cassette in intron 3, creating a null allele ($Rb^{\times 3t}$). For the second allele, a targeting vector carrying a puro cassette and *lox*P sites (open triangles) was used ($Rb^{\times 3loxPuro}$ allele). Upon introduction of Cre, *Rb* exon 3 was deleted, creating a null allele ($Rb^{\times 3\Delta}$). The boxes marked E and I represent the two probes used in the Southern blot analysis, and the arrows marked 1, 2, and 3 represent the primers used in the PCR analysis. N, *Nco*1; P, *Pst*1; K, *Kpn*1; S, *Sal*1. Not to scale. (*B*) Southern blot analysis of TKO ES cells. Genomic DNAs of $p107^{-/-};p130^{-/-}$ ES cells with various *Rb* alleles were digested with *Nco*1 and *Sal*1 and hybridized with probe E (left panel) or with *Pst*1 and *Kpn*1 and hybridized with probe I (right panel). Arrows indicate alleles. The ES cells are on a mixed C57BL/6x129Sv genetic background, and the *Nco*1–*Sal*1 digest provides a polymorphism allowing us to distinguish both *Rb* alleles. (*C*) TKO MEF populations purity assayed by PCR. Primers 1–2 and 1–3 amplify *Rb* wild-type (wt) and mutant (mut) alleles, respectively (Williams et al. 1994). At passage 0 (P0), TKO MEFs are mixed with wild-type MEFs. After selection, at passage 2 (P2), contaminating wild-type cells are absent. Three representative examples of TKO MEF populations are shown, as well as amplification results from control ES cells DNAs. (*D*) Western blot analysis of the three pRB family members in MEFs bearing different combinations of mutant alleles in *Rb*, *p107*, and *p130*. Two TKO MEF lines from two independent ES cells clones are shown. (*E*) E2F electromobility shift assays using extracts from exponentially growing TKO and control MEFs. p107 and p130 antibodies shift p107:E2F and p130:E2F complexes in $Rb^{-/-}$ cells, and pRB antibody shifts pRB:E2F complexes in $p107^{-/-};p130^{-/-}$ cells. In contrast, in TKO cells, no complex is visible or shifted by these antibodies, and only the E2F-4 antibody shifts free E2F.* indicates a nonspecific complex. The probe has been run off the gel for better resolution. Bound and free (in complexes with pRB family or not) E2F are indicated as well as supershifts. When indicated, a 1000 times excess of specific competitor was added in the reactions.

in the coding sequence and, therefore, if stable, only the extreme N-terminal part of the pRB protein could be expressed from this $Rb^{\times 3\Delta}$ allele (see below). Exponentially growing undifferentiated TKO ES cells were indistinguishable from control ES cells (data not shown), which is consistent with an apparent lack of pRB regulation in ES cells (Savatier et al. 1996).

TKO MEFs were obtained from chimeric embryos produced via blastocyst injection of different TKO ES cells clones. After plating, the mutant MEFs were selected for two passages in culture using neomycin and hygromycin, and elimination of contaminating wild-type MEFs was assessed by genomic PCR (Fig. 1C). To ensure that the selection process did not alter the properties of TKO

MEFs, $Rb^{-/-}$ and $p107^{-/-};p130^{-/-}$ control MEFs lines were also generated from chimeric embryos following the same protocol. Control MEFs prepared by this method had similar growth properties in culture to cells prepared directly from germ-line mutant embryos. $Rb^{-/-}$ and $p107^{-/-};p130^{-/-}$ MEFs were chosen as controls because these cells have been previously characterized in various cell-based assays (Herrera et al. 1996; Hurford et al. 1997; Samuelson and Lowe 1997; Brugarolas et al. 1998; Harrington et al. 1998) and because p107 and p130 proteins are more closely related to each other than they are to pRB (Weinberg 1995). It is important to note that we have not compared the TKO cells to all double-mutant combinations (see Discussion). As determined by Western blot analysis, TKO MEFs did not express any of the *pRb* family proteins, whereas $p130^{-/-};p107^{-/-}$ MEFs express only pRB and $Rb^{-/-}$ MEFs express both p107 and p130 (Fig. 1D). Similarly, in E2F gelshift assays, $p107^{-/-};p130^{-/-}$ and $Rb^{-/-}$ MEFs extracts contained both E2F and free E2F complexes bound to pRB family proteins, which could be supershifted with specific antibodies (Fig. 1E). In TKO MEFs, the addition of antibodies directed against the three family members did not alter the gelshift pattern (Fig. 1E). This experiment confirms that TKO cells do not express any known pRB family protein and indicates that they possess high levels of E2F in the free form. We also failed to reproducibly observe distinct E2F-containing complexes in the TKO MEFs, although given the limitation of the assay, these data do not conclusively rule out the existence of additional pRB-related protein (see Discussion). In conclusion, these results show that TKO MEFs (and ES cells) are viable and proliferate in culture, demonstrating that pRB, p107, and p130 are dispensable for basic cell cycle progression and cellular survival under these conditions.

Initial cell cycle characterization of TKO MEFs

According to the model in which the pRB family proteins control cell cycle entry by inhibiting the action of E2F, the absence of pRB, p107, and p130 would be expected to have an effect on the G_1/S transition of the cell cycle. Flow cytometric analysis performed on cells cultured in 10% serum showed that ~20% of exponentially growing wild-type, $p107^{-/-};p130^{-/-}$ and $Rb^{-/-}$ MEFs were in the S phase of the cell cycle, whereas under the same conditions, close to 35% of TKO MEFs were in S phase (Fig. 2A). Associated with an increased S-phase fraction, TKO MEFs also had a pronounced decrease in the percentage of cells in G_1 (43% versus 63% for wild-type cells).

An acceleration of the G_1 phase and/or the G_1/S transition would be expected to reduce overall cell cycle times. Therefore, we examined TKO and control MEFs

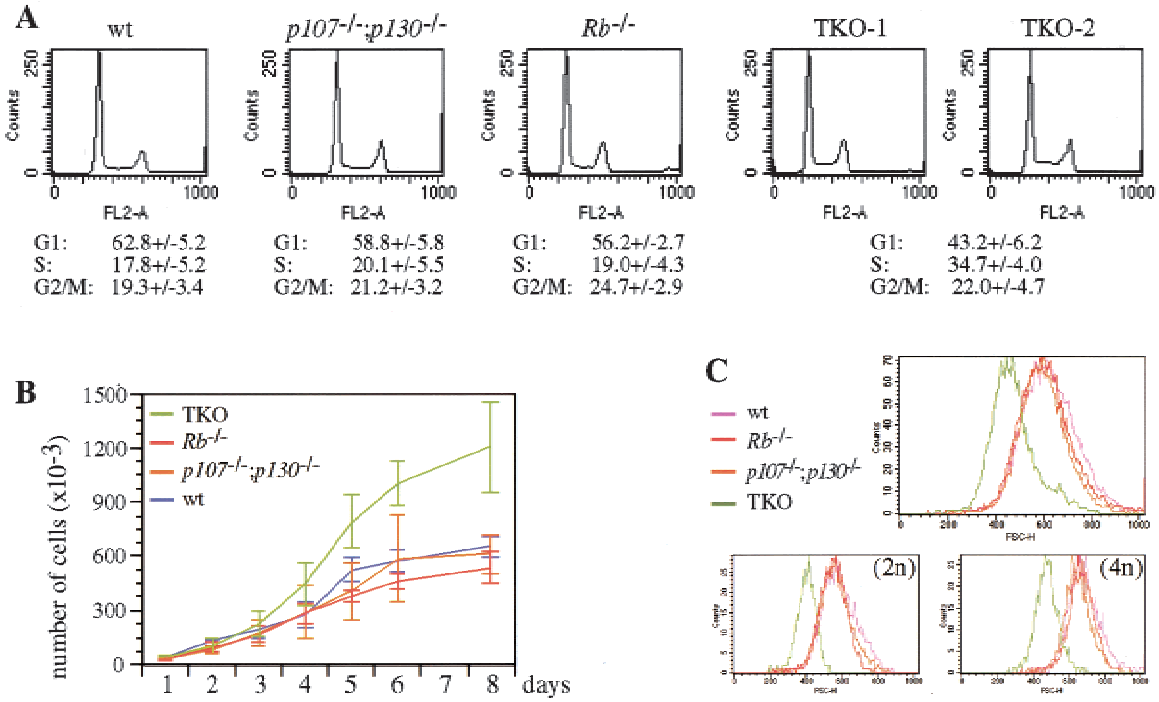

Figure 2. Cell cycle analysis of TKO and control MEFs. (*A*) Flow cytometric cell cycle analysis of representative wild-type (wt), $Rb^{-/-}$, $p107^{-/-};p130^{-/-}$, and TKO MEF cultures. G_1, S, and G_2/M populations are indicated as percentages of the whole population. Numbers correspond to the average of at least five independent experiments, with standard deviations (+/–). (*B*) Proliferation curves of TKO and control MEFs. The curves represent the average of three experiments for control MEFs and five for TKO MEFs, with standard deviations (error bars). (*C*) Cell size analysis of TKO and control MEFs. Asynchronously proliferating cells fixed and stained with PI were analyzed by flow cytometry. Populations were gated in a FSC-H by FL2-A dot plot and scored in a FSC-H histogram. The top panel represents whole populations and the two bottom panels 2n and 4n populations, as indicated.

for their proliferation rates. In the exponential phase of proliferation (2–4 d after plating; Fig. 2B), the population doubling time of TKO MEFs was 20%–25% shorter than control cells (24 h versus 28–30 h). These data confirm our previous report that the overall doubling time of $Rb^{-/-}$ MEFs is similar to that of wild-type MEFs even though they have a shorter G_1 phase (Herrera et al. 1996) and indicates that the cell cycle defects in TKO MEFs are more profound. The viability of exponentially growing wild-type, $Rb^{-/-}$, $p107^{-/-};p130^{-/-}$, and TKO cells were close to 95% and not significantly different, as assayed by Trypan blue exclusion and annexin staining (data not shown).

When cells reach confluence, after 6–8 d in culture, TKO MEFs were two to three times more abundant than the controls (Fig. 2B). When examined in light microscopy, TKO cells were notably small in size (not shown), and FACS analysis measuring forward-side scatter indicated that they were ~40%–50% smaller than control cells by volume (Fig. 2C). We have previously reported that $Rb^{-/-}$ MEFs have a slightly reduced volume compared to wild-type cells, but only in the 2n population (Brugarolas et al. 1998). However, both the 2n and 4n populations of TKO MEFs had reduced volume (Fig. 2C), which is again indicative of a more profound cell cycle defect.

TKO cells do not arrest in G_1 following exposure to DNA-damaging agents

The cell cycle properties of TKO MEFs suggest a significant defect in G_1 control. The response to DNA damage is a commonly used measure of G_1 regulation in mammalian cells, and defects in this response are important in tumor progression (Kastan 1997). Wild-type MEFs respond to the DNA damage caused by γ irradiation by inducing a p53-dependent G_1 arrest and a p53-independent G_2 arrest (Kastan et al. 1992). The G_1 arrest response in MEFs has been shown to be partially dependent on the presence of functional pRB (Samuelson and Lowe 1997; Harrington et al. 1998). Therefore, we tested the response of TKO and control cells to γ irradiation. As expected, wild-type MEFs accumulated in G_1 by 18 hours after γ irradiation (Fig. 3A). $Rb^{-/-}$ and $p107^{-/-}$; $p130^{-/-}$ MEFs appear to have a reduced G_1 arrest response, as described previously for $Rb^{-/-}$ MEFs. Strikingly, TKO MEFs, like $p53^{-/-}$ MEFs, were completely deficient for the G_1 arrest response (Fig. 3A). Also similar to $p53^{-/-}$ MEFs, TKO cells accumulated in G_2/M following γ irradiation.

We also treated MEFs of different genotypes with the chemotherapeutic agent, doxorubicin, which causes double-strand breaks and other forms of DNA damage and causes G_1 arrest in wild-type MEFs (L. Attardi, A. de Vries, T. Jacks, in prep.). As with γ irradiation, TKO cells failed to arrest in G_1 and accumulated in the G_2/M phase of the cell cycle (Fig. 3B). As expected, $p53^{-/-}$ MEFs were also blocked in G_2/M following doxorubicin treatment. $Rb^{-/-}$ and $p107^{-/-};p130^{-/-}$ MEFs displayed an intermediate phenotype (Fig. 3B), with partial arrest in G_1.

These experiments implicate *p107* or *p130* in the cellular DNA damage-response pathway, as previously suggested in experiments using the HPV E7 oncoprotein (Demers et al. 1994; Slebos et al. 1994), but in contrast to previous observations in $p107^{-/-};p130^{-/-}$ MEFs (Harrington et al. 1998). More generally, they demonstrate that multiple members of the pRB family are required for proper cell cycle arrest following DNA damage. The normal DNA damage response has been shown previously to be dependent on p53 and its target gene $p21^{CIP1}$ (Dulic et al. 1994; Brugarolas et al. 1995). Western blot analysis of TKO cells showed that p53 was expressed at high levels in TKO MEFs (Fig. 3C). The p53 protein was shown to be functional in electromobility shift analysis (data not shown), and importantly, following doxorubicin treatment (Fig. 3D) and γ irradiation (data not shown), the expression of the p53 target gene $p21^{CIP1}$ was induced in TKO cells. Therefore, we conclude that the $p53/p21^{CIP1}$ cell cycle arrest pathway induced following DNA damage converges on the pRB family proteins.

TKO cells do not arrest in G_1 following contact inhibition and serum starvation

In addition to the fact that they are smaller, TKO MEFs might have reached a higher density at confluence (Fig. 2B) if they were not sensitive to contact inhibition (Holley 1975). When left at confluence for 2–3 d, even when media was replenished daily, wild-type, $p107^{-/-};p130^{-/-}$, and $Rb^{-/-}$ MEFs showed a typical G_0/G_1 cell cycle arrest. In contrast, TKO MEFs did not undergo cell cycle arrest under these conditions (Fig. 4A) and showed increased cell death (data not shown; see below). We next performed a modification of this experiment, in which after 2 d at confluency, the medium was changed to 0.1% serum for two additional days. Under these conditions, wild-type MEFs were fully arrested in G_0/G_1, without a significant increase in cell death (Fig. 4B–D; see Brugarolas et al. [1998] for $Rb^{-/-}$ cells). In striking contrast, low serum concentrations resulted in a massive cell death of confluent TKO MEFs cultures. A representative example of confluent TKO cells dying in 0.1% serum is shown in Figure 4B, where a sub-G_1 population is visible in the FACS population, indicative of cells with degraded genomic DNA. Western blot analysis using antibodies directed against a cleaved form of the PARP protein performed on these cell extracts confirmed that the TKO cells, but not the controls, were dying from apoptosis (Fig. 4C). Annexin staining of the cells indicated that only 20%–30% of TKO cells were still alive in these conditions (Fig. 4D). When dead cells were carefully removed from the starved, confluent TKO MEF populations, the remaining cells were shown to be in active cell cycle (Fig. 4C). Similarly, decreased growth factors concentrations in nonconfluent TKO cell cultures resulted in high levels of apoptosis and no G_0/G_1 arrest (data not shown). These experiments indicate that presence of the three family members is necessary to enable the cells to arrest in G_1 following cell–cell contact and serum withdrawal, as was the case for DNA damage response. In

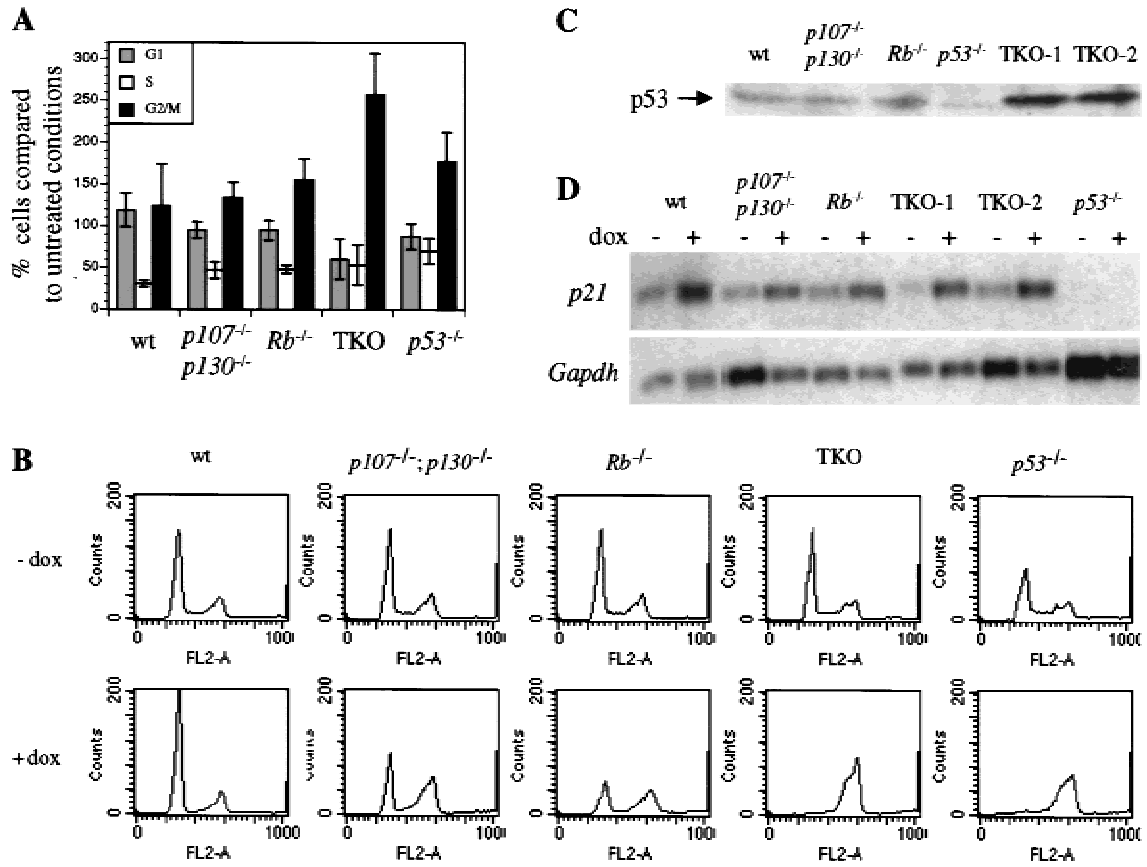

Figure 3. Response of TKO and control MEFs to DNA damaging agents. (*A*) Cell cycle analysis of TKO and control MEFs following γ irradiation. Cell populations were sorted by flow cytometry in G_1, S, and G_2/M phases 18 h after irradiation. Numbers are relative to numbers obtained for nonirradiated cells, and standard deviations are indicated (error bars). (*B*) Cell cycle analysis of TKO and control MEFs following doxorubicin (dox) treatment. Representative flow cytometry results are shown for all the genotypes 18 h after treatment. The experiment was repeated at least three times with similar results. Panels for treated (+dox) and untreated (–dox) cells are aligned to show the variations in the G_1, S, and G_2/M populations. (*C*) Western blot analysis of p53 levels in exponentially growing TKO and control cells. (*D*) Northern blot analysis of $p21^{CIP1}$ expression in MEFs from different genotypes following DNA damage. RNAs were prepared from cells treated/not treated with doxorubicin (+/– dox). After hybridization with a *p21* cDNA probe, the same blot was rehybridized with a *Gapdh* probe to control loading.

contrast to the DNA damage response, however, TKO cells failed to arrest in G_2/M under these conditions and underwent apoptosis. In this respect, these results implicate *p107* and *p130* in the inhibition of apoptosis.

TKO MEFs are immortal

An important step in cellular transformation is the ability to grow indefinitely by bypassing the normal senescence program that imposes a finite number of divisions in culture. Given that senescence results in G_1 arrest and that TKO MEFs have defective G_1 arrest responses, we examined the lifespan of these cells in culture using the 3T3 protocol (Todaro and Green 1963). In eight independent experiments using cells derived from different chimeric embryos, TKO MEFs maintained constant proliferation rates and failed to undergo senescence (Fig. 5A). The absence of the senescence phenotype in these cells was confirmed by examining individual cells microscopically, where no morphological changes associated with senescence (flat, large, nondividing cells) were observed (data not shown). $p53^{-/-}$ MEFs, which have been shown to be immortal (Harvey et al. 1993), served as positive controls in this experiment. In contrast, 5 of 6 wild-type, six of eight $p107^{-/-};p130^{-/-}$, and three of five $Rb^{-/-}$ MEF cultures underwent senescence in the 3T3 protocol, and cells from these cultures showed features of senescence (Fig. 5A; data not shown). Importantly, those control MEFs that gave rise to immortalized cells showed a typical biphasic proliferative curve over time. In the first phase of the curve, the population doubling times decreased regularly as the bulk of the cells underwent senescence. These cultures then expanded again at later passages, consistent with the emergence of an immortalized clone(s) following a subsequent genetic event(s).

Another measure of cellular immortalization is growth at very low cell density, which triggers a rapid or

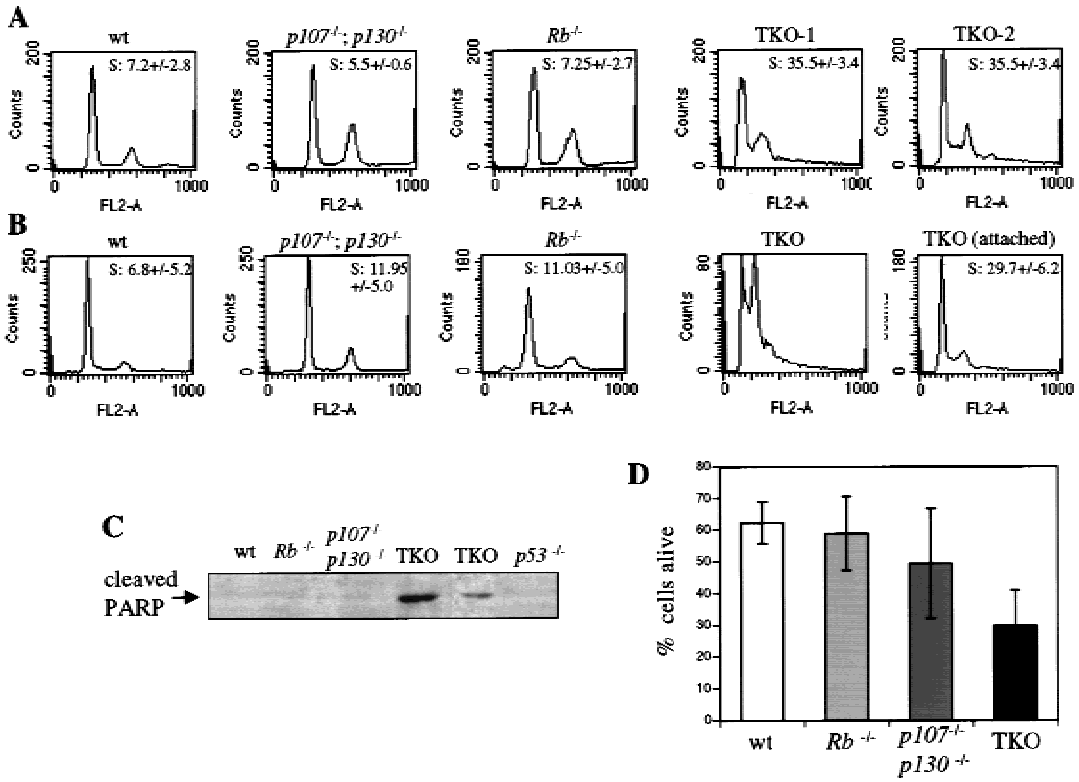

Figure 4. Response of TKO and control MEFs to cell–cell contact and low serum conditions. (*A*) Cell cycle analysis of confluent TKO and control MEFs. One or two representative results are shown for each genotype. The percentage of cells in the S phase of the cell cycle is indicated, with standard deviations (+/–). At least three experiments were performed. (*B*) Cell cycle analysis of confluent TKO and control MEFs in 0.1% serum. The percentages of cells in the S phase of the cell cycle are indicated, with standard deviations (+/–). At least three experiments were performed. "TKO" represents an experiment where all the cells, attached to the plate or floating, were included in the assay. No S-phase count was calculated in these conditions given the high sub-G_1 population. Control cells were analyzed in the same way. "TKO (attached)" corresponds to an experiment where floating cells were removed before cell cycle analysis. (*C*) Western blot analysis of the cleaved form of PARP specific of apoptotic cells in confluent TKO and control cells grown in 0.1% serum. Extracts were prepared from whole populations, including dead, floating cells. (*D*) Survival of confluent MEF populations grown in 0.1% serum. Annexin negative and positive cell populations were sorted by flow cytometry, and annexin negative cells were considered to be alive. Percentages are the average of at least three experiments, with standard deviations (error bars).

premature senescence program in wild-type MEFs. In contrast to control MEFs, we found that when plated at low density, TKO MEFs were able to proliferate and form colonies (Fig. 5C), a process similar to but not performed as efficiently as $p53^{-/-}$ MEFs. As in the DNA damage and 3T3 experiments, $Rb^{-/-}$ MEFs showed an intermediate response in this assay, with more colonies growing after plating at low density than with wild-type MEFs.

To ensure that TKO cells had not accumulated mutations that led to a bypass of the senescence program before the immortalization assays, we examined the sensitivity of the cells to ectopic expression of pRB. Early-passage TKO MEFs were infected with a retrovirus expressing a wild-type human *RB* cDNA before low-density plating. Expression of pRB was verified in these cells by Western blot analysis (data not shown). As shown in Figure 5D, reexpression of pRB in TKO cells inhibited the colony formation completely. This result demonstrates that TKO cells remain sensitive to pRB family function under these conditions and indicates that their immortalized state is a direct result of the lack of these proteins.

Among many changes associated with senescence in culture, increased expressions of the cell cycle inhibitors $p16^{INK4A}$ and $p19^{ARF}$ are thought to be critical in inducing permanent G_0/G_1 arrest (Kamijo et al. 1997; Stein and Dulic 1998). Importantly, similar to wild-type cells, the levels of $p16^{INK4A}$ and $p19^{ARF}$ increased in later passages TKO cells (Fig. 5B). Thus, TKO cells appear to be resistant to growth arrest signals induced by elevated $p16^{INK4A}$ and $p19^{ARF}$ levels.

The $p21^{CIP1}$ cell cycle inhibitor has also been shown to play a role similar to that of $p16^{INK4A}$ in senescence in human cells, although its role in mouse cells is less clear (Brown et al. 1997; Pantoja and Serrano 1999). In early passages of TKO MEF cultures during the 3T3 protocol, $p21^{CIP1}$ levels remained constant or increased as expected (Fig. 5B). Interestingly, however, $p21^{CIP1}$ levels strongly decreased in two of five late-passage TKO MEF cultures tested (Fig. 5B). Given that $p21^{CIP1}$ is a direct

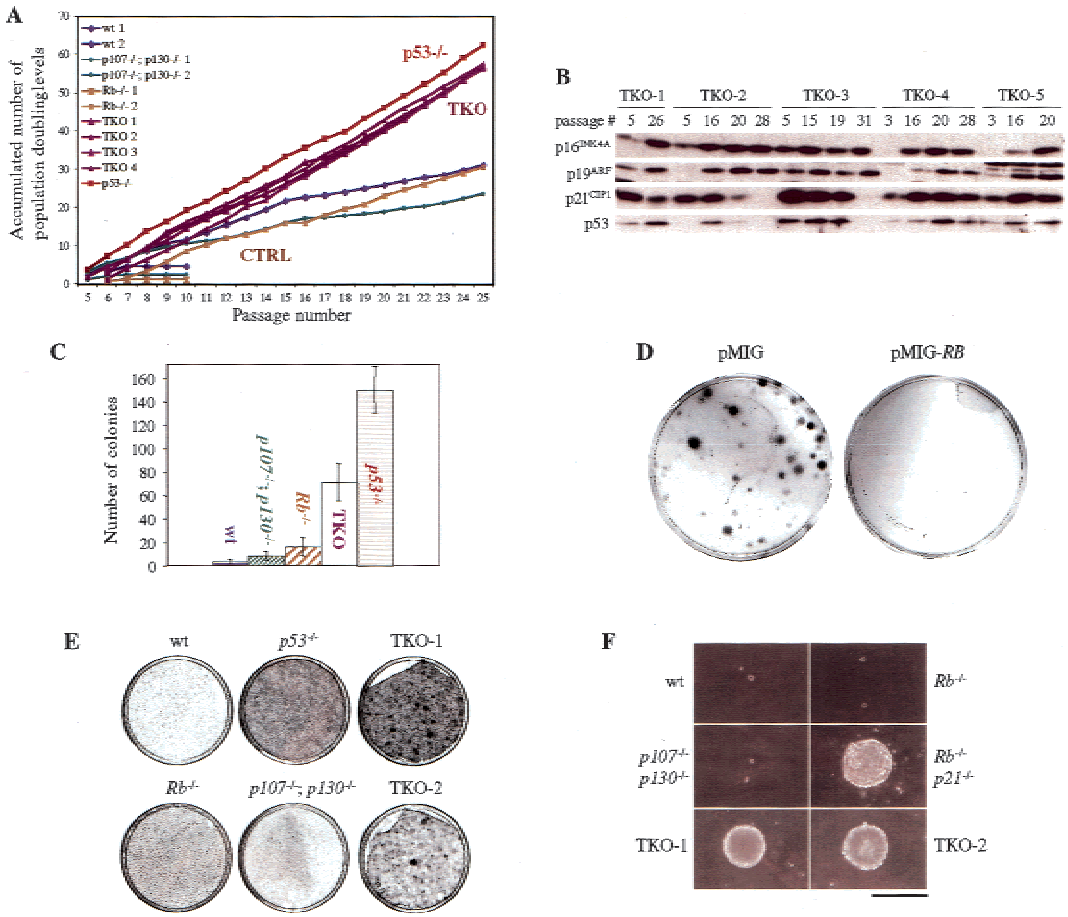

Figure 5. Immortality and partially transformed phenotype of TKO MEF populations. (*A*) Cultures derived from individual embryos were cultivated according to the 3T3 protocol. The graph shows the accumulated number of doublings that representative cultures have undergone. Full legend is as indicated in the graph. Groups of MEFs with the same genotypes or phenotypes are also indicated (CTRL, controls: wt, $Rb^{-/-}$ and $p107^{-/-};p130^{-/-}$). (*B*) Western blot analysis of p53 and of $p16^{INK4A}$, $p19^{ARF}$, and $p21^{CIP1}$ cell cycle inhibitors in early and late passage TKO clones. TKO cells (1–5) extracts were prepared at different passages, as indicated. Equal quantities of proteins were analyzed. (*C*) Proliferation of TKO and control cells after plating at low density. 1.3×10^3 cells of each genotype were plated per 10-cm plate, and after 2 wk, colonies were stained and counted. At least five experiments were performed; average numbers and standard deviations (error bars) are shown. (*D*) TKO cells were infected with an empty retrovirus (pMIG) or with the same retrovirus expressing a human *RB* cDNA (pMIG-*RB*) and then plated at low density. The plates were stained with Giemsa to visualize the colonies 2 wk after plating. (*E*) Representative examples of TKO and control MEFs grown for 2 wk at confluency. TKO cells form a very dense layer with foci growing on top of it and with a tendency to peel off the plate. This phenomenon was not observed with wt, $Rb^{-/-}$, $p107^{-/-};p130^{-/-}$, and $p53^{-/-}$ cells. (*F*) Ability of MEFs with different genotypes to form colonies in soft agar. Pictures were taken at the same magnification (bar, 400 μm) after 24 d in culture.

target of p53, we examined p53 levels in early- and late-passage TKO cells. Initially, p53 levels remained constant or increased in TKO MEF cultures over time (Fig. 5B). However, p53 levels decreased significantly in the two late-passage TKO MEF cultures that showed reduced $p21^{CIP1}$ expression (Fig. 5B). These data indicate that while loss of p53 function is not required for the immortalization of TKO cells per se, *p53*-deficient variants might be selected following prolonged passages, perhaps because of reduced apoptotic rates in these cells. Consistent with the lack of requirement of p53 mutation for immortalization in TKO MEFs, we observed persistent expression of $p21^{CIP1}$ and p53 in all clones ($n = 12$) originating from low-density plating of two independent TKO MEF cultures (data not shown). Together, these results indicate that TKO cells are immortal and resistant to signals controlling senescence in MEFs and that loss of the three pRB family members is sufficient to bypass the senescence program.

Focus formation, anchorage-independent proliferation, and Ras transformation of TKO MEFs

On the basis of the various assays described above, TKO MEFs share many properties of transformed cells. To characterize the state of transformation of these cells further, we examined two well-studied features of transformation, focus formation on a monolayer of cells and

anchorage-independent proliferation, as well as sensitivity to oncogenic Ras expression. As shown in Figure 5E, TKO cells were able to form foci on top of a confluent monolayer of cells after 2–3 wk of culture, a phenomenon not observed in control cells. Interestingly, $p53^{-/-}$ MEFs behaved similarly to wild-type MEFs in these assays, arresting in G_0/G_1 on confluency and failing to form spontaneous foci (Fig. 5F). Transformed cells originating from adherent cells commonly show the ability to grow in anchorage-independent conditions (Assoian and Zhu 1997). We found that TKO MEFs also exhibited this aspect of transformation, as evidenced by their ability to form colonies in soft agar. The extent of growth of TKO cells was comparable to that of $Rb^{-/-};p21^{-/-}$ MEFs (Brugarolas et al. 1998), while none of the control genotypes were able to form colonies in soft agar (Fig. 5F). In these experiments, however, TKO MEFs were not as robust as $p53^{-/-}$ cells transformed with oncogenic Ras and adenovirus E1A, which formed more and larger foci and soft-agar colonies (data not shown; see Brugarolas et al. 1998). Thus, although they possess some features of transformed cells, TKO MEFs are not fully transformed. Indeed, when injected into the flank of nude mice, they failed to form tumors (Table 1).

To examine the effects of oncogenic Ras expression on TKO MEFs, cells were infected with a retrovirus carrying the oncogenic H-RasV12 and subjected to selection to obtain pure populations. As described previously (Serrano et al. 1997), wild-type MEFs underwent a form of cellular senescence on overexpression of activated Ras, as did $Rb^{-/-}$ and $p107^{-/-};p130^{-/-}$ MEFs (data not shown). In contrast, TKO MEFs expressing H-RasV12 exhibited a dramatic change in morphology, indicative of transformation, and continued proliferating after several weeks and several passages in culture (Fig. 6A,B). In addition, compared to TKO cells, these H-RasV12-TKO cells formed more clones after plating at low density (Fig. 6C), produced larger foci in confluent cultures (data not shown), and showed enhanced proliferation in soft agar (Fig. 6D). Furthermore, H-RasV12-TKO MEFs were tumorigenic in nude mice (Table 1). Thus, oncogenic Ras can cooperate with inactivation of the three pRB family members in cellular transformation, including by promoting tumorigenic potential (see Discussion).

Table 1. *Cooperation of* Rb *family inactivation with oncogenic Ras in a nude-mice transformation assay*

MEFs genotype	Tumors	Number of different clones tested
Wild-type	0/2	2
$p107^{-/-};p130^{-/-}$	0/4	2
$Rb^{-/-}$	0/4	2
TKO	0/6	4
$p53^{-/-}$	0/2	2
*H-Ras*V12-TKO[a]	8/10	6
*H-Ras*V12;*E1A*;$p53^{-/-}$[b]	3/3	1

Each clone was injected one or two times.
[a]Tumors apparent 12–15 d after injection into nude mice.
[b]Tumors apparent 8–10 d after injection into nude mice.

Discussion

Convergence of growth arrest signals on the Rb family

We show here that mouse embryonic fibroblasts mutants for the three pRB family members are unable to arrest in G_1 following various inhibitory signals, such as confluence, low serum, detachment from the substratum, DNA damage, or normal or premature senescence. All of these signals use different transduction pathways to induce cell cycle arrest, but eventually, each is thought to converge on the cell cycle inhibitors of the INK4 and/or CIP/KIP families. For example, it is known that the senescence program involves increased levels of both $p16^{INK4A}$ and $p21^{CIP1}$ (Stein and Dulic 1998) and that low-serum conditions inhibit cyclin D1– and cyclin E–dependent kinases activities via $p16^{INK4A}$ and $p21^{CIP1}$/$p27^{KIP1}$, respectively (Sherr 1996). Our data would indicate that absence of the pRB family eliminates key targets of these inhibitors and makes cells refractory to G_1 arrest. Preliminary observations indicate that TKO cells are also resistant to G_1 arrest induced by overexpression of $p27^{KIP1}$ and $p19^{ARF}$ cell cycle inhibitors (J. Sage and K. Tsai, unpubl.). It will be interesting to determine whether any conditions that normally induce G_1 arrest would operate in cells lacking pRB family function.

Immortalization

It has been postulated that cells in which G_1 control was compromised may undergo inappropriate S-phase entry, accumulate mutations, and undergo cellular transformation (Pardee 1989; Sherr 1996). We show here that absence of pRB family function and consequent loss of G_1 control leads to cellular immortalization directly. 3T3 assays, low-density plating experiments, and absence of senescence induced by oncogenic Ras have been used previously to demonstrate the immortalized properties of $Ink4a^{-/-}$, $ARF^{-/-}$, and $p53^{-/-}$ MEFs (Harvey et al. 1993; Kamijo et al. 1997; Serrano et al. 1997). Thus, the still-to-be-defined signal transduction pathway that leads from excessive mitogenic signaling or prolonged passage in culture to increased levels of $p16^{INK4A}$, $p19^{ARF}$, p53, and $p21^{CIP1}$ converges on the pRB family. Also, in cells lacking just pRB or just p107 and p130, the senescence programs can effectively result in permanent G_0/G_1 arrest; in cells lacking all three proteins, such programs are ineffective.

Cellular transformation

We have shown here that inactivation of the pRB family is not sufficient for full cellular transformation. For example, TKO MEFs are not tumorigenic in nude mice, and their ability to form colonies in soft agar or to form foci at confluency is reduced compared to fully transformed cells. This suggests that loss of G_1 control leads to immortalization but is not sufficient for full transformation and that additional mutations are required for this effect. We have observed that TKO cells are more

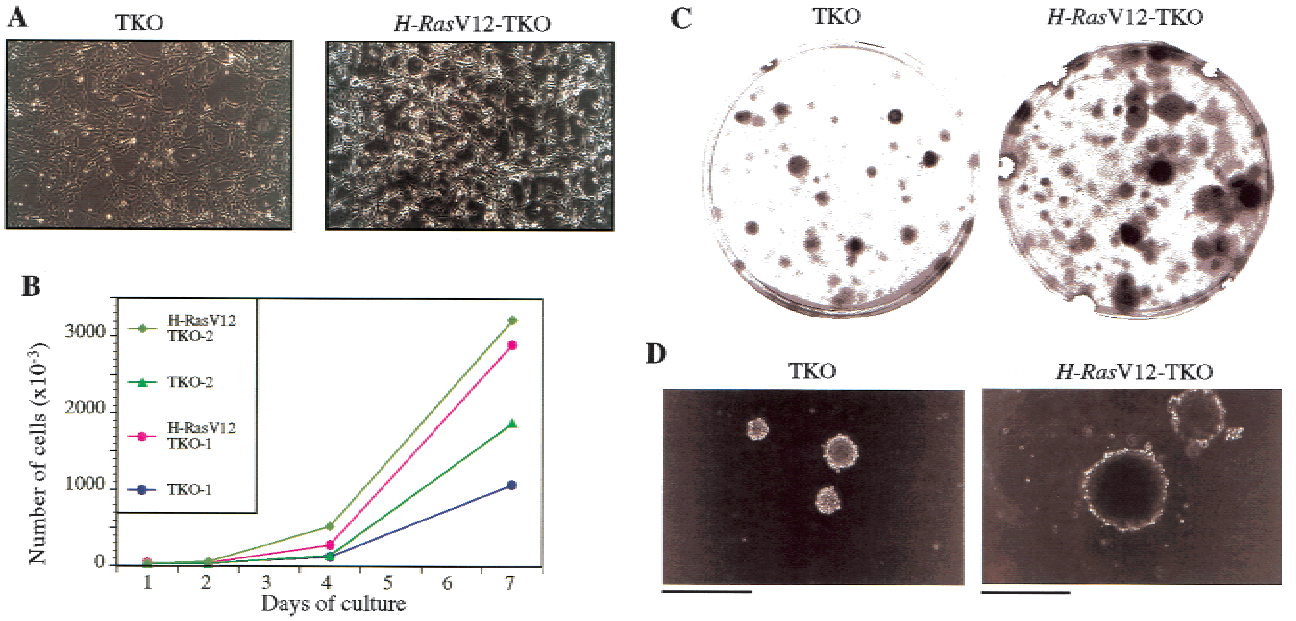

Figure 6. Properties of H-RasV12-TKO MEFs. (*A*) Morphological changes induced by activated Ras in TKO MEFs. Left panel shows TKO MEFs infected with a pBabe empty retroviral vector, and right panel shows the same TKO MEFs clone infected with a pBabe-H-RasV12 vector. Photomicrographs were taken 2 wk after infection and selection (magnification 100×). No indications of premature senescence are observed in H-RasV12-TKO cells. (*B*) Representative proliferation curves of H-RasV12-TKO MEFs. H-RasV12-TKO MEFs continue to proliferate 2 wk after infection and selection, whereas under similar conditions H-RasV12 control MEFs (wild-type, $Rb^{-/-}$ and $p107^{-/-};p130^{-/-}$) undergo senescence (data not shown). (*C*,*D*) Representative examples of the enhanced ability of H-RasV12-TKO cells to form colonies 2 wk after plating at low density (*C*) or in soft agar (*D*), compared to TKO cells infected with a pBabe empty vector (TKO; bar 400 μm).

susceptible than control cells to cell death under specific conditions and, also, that loss of p53 occurred in some late-passage TKO cultures. Thus, antiapoptotic mutations might cooperate with pRB family mutations in transformation. In addition, oncogenic Ras caused increased tumorigenicity of TKO cells, suggesting that increased mitogenic signaling can promote transformation in cells lacking G_1 control. It must be noted, however, that Ras-transformed $p53^{-/-}$ MEFs or NIH3T3 cells form larger colonies in soft agar and tumors in nude mice more rapidly than Ras-transformed TKO cells. Therefore, mutations in other cellular pathways may be required for full transformation.

Functional overlap

The analysis of TKO and control MEFs underscores the degree of functional overlap between the three pRB family members and indicates that this overlap is present in many aspects of cell cycle regulation. Depending on the assay, $Rb^{-/-}$ or $p107^{-/-};p130^{-/-}$ cells were either indistinguishable from wild-type cells (e.g., colony formation in soft agar or Ras-induced senescence) or showed an intermediate response between wild-type and TKO MEFs (e.g., G_1 length or response to DNA-damaging agents). Therefore, the degree to which different pRB proteins can functionally compensate for one another may vary depending on the cellular context. The phenotypic differences between $Rb^{-/-}$ and TKO cells highlight the importance of p107 and p130 as cell cycle regulators, at least in cells with compromised pRB function. It is also possible that in certain conditions, p107 or p130 are more functionally related to pRB than they are to each other, and therefore, one might expect additional intermediate phenotypes in $Rb^{-/-};p107^{-/-}$ or $Rb^{-/-};p130^{-/-}$ cells. Indeed, Dannenberg et al. (2000) report that $Rb^{-/-};p107^{-/-}$ MEFs are immortal.

Lack of additional Rb family members

On the basis of experiments performed in $p107^{-/-};p130^{-/-}$ MEFs and T lymphocytes, we and others had suggested that an additional E2F binding protein might be present in mouse cells (Hurford et al. 1997; Mulligan et al. 1998). Specifically, a fraction of cellular E2F was found in a complex that could not be supershifted with anti-pRB antibodies in these cells. However, in the analysis of TKO MEFs grown in various conditions (e.g., low serum concentration, confluence treatment, exposure to DNA-damaging agents), we have no compelling evidence for such an activity (Fig. 1E; data not shown). It is possible that in both previous reports, the pRB-specific antibodies failed to supershift all of the pRB-containing complexes. However, because of the limitations of electromobility shift assays, novel E2F complexes might not have been detected in these cells under these conditions.

Finally, to date we have failed to identify additional pRB-related proteins on searching EST and genomic sequence databases. The availability of the complete human and mouse genome sequences will allow for a definite conclusion to this point.

Control of the cell cycle upstream and downstream of the pRB family

The availability of cells carrying combined mutations for the pRB family members and the knowledge of the upstream and downstream regulatory pathways that affect them allow for a better understanding of the similarities and differences between the three family members. However, several points still remain unclear. For example, ectopic expression of $p16^{INK4A}$ does not induce G_1 arrest in $Rb^{-/-}$ cells (Medema et al. 1995). This result is difficult to reconcile with our current understanding of functional compensation within the *Rb* family. Perhaps the residual cell cycle regulation provided by p107/p130 is not sufficient to confer growth arrest in this setting. In addition, it has recently been shown that $p16^{INK4A}$ overexpression does not arrest $p107^{-/-};p130^{-/-}$ cells (Bruce et al. 2000). It is, therefore, possible that in some circumstances a certain threshold level of activation of the pRB family function is necessary for proper cell cycle arrest and that the level of this threshold may vary depending on the cellular context.

The E2F family of transcription factors can be divided in two groups, with E2F-1, E2F-2, and E2F-3 serving as activators of transcription and E2F-4 and E2F-5 being involved primarily in transcriptional repression through recruitment of pRB family proteins. pRB, p107, and p130 interact differentially with the E2F family proteins: pRB binds preferentially to the E2F-1–4, and p107 and p130 interact more specifically with E2F-4 (Dyson 1998). These differences suggest that the pRB family members control two types of downstream pathways to arrest cells, perhaps targeting two different sets of genes. However, the target genes of the E2F family have not been well characterized, and little information exists concerning the specificity of each member of this family. Availability of E2F mutant cells in combination with *Rb* family mutations will permit investigation of these issues (Tsai et al. 1998; Yamasaki et al. 1998).

Human cancer

Our observations with TKO cells raise the question of the importance of *p107/p130* mutations in human cancer. Mutations in these genes have been found only rarely and in a small subset of tumor types (Takimoto et al. 1998; Claudio et al. 2000). In contrast, many human tumor types exhibit structural mutations in *RB* itself (Goodrich and Lee 1993; Weinberg 1995). Thus, with respect to human tumorigenesis, loss of pRB function alone would appear to confer a selective advantage. This situation may resemble the $p16^{INK4A}$-induced growth arrest in MEFs, where *Rb* mutation is sufficient to confer insensitivity. In other circumstances, however, loss of pRB family function as a whole may lead to some additional proliferation advantage. This may coincide with mutations in genes that regulate pRB, p107, and p130, such as *INK4A* or *CDK4* (Weinberg 1995). In support of this possibility, some human tumors have been described to have *RB* mutation and CDK4 amplification or mutations in both *RB* and *P16INK4A* (Ruas and Peters 1998). Further mutational analysis in human cancer as well as the study of the tumorigenic potential of mouse cells carrying compound mutations in the pRB family will help to resolve this issue.

Materials and methods

Culture of ES cells

ES cells were grown as described (Jacks et al. 1992). $p107^{-/-}$; $p130^{-/-}$ ES cell lines were derived from blastocysts (Robertson 1997) produced by crossing $p107^{-/+};p130^{-/-}$ mice on a mixed C57BL/6;129/Sv genetic background (Cobrinik et al. 1996; Lee et al. 1996). After electroporation with the targeting vectors, ES cells were selected with 150 µg/mL hygromycin (Roche) or 2.5 µg/mL puromycin (Sigma). To delete the sequences flanked by *lox*P sites (see Fig. 1A), ES cells were coelectroporated with a Cre-expressing plasmid (a gift from B. Sauer, Oklahoma City, OK) and a plasmid expressing the zeocin resistance gene (Invitrogen). ES cells were selected for 48 h with 20 µg/mL zeocin 24 h after electroporation. This brief selection did not kill nonelectroporated cells but slowed their growth, leading to enrichment in clones transiently expressing Cre.

Targeting vectors for homologous recombination

Targeting of the first *Rb* allele in $p107^{-/-};p130^{-/-}$ ES cells was performed as described (Williams et al. 1994). For the second allele, a new *Rb* targeting vector was constructed with an additional 4.7-kb fragment of the *Rb* genomic locus on the 5′ arm to improve the targeting efficiency and with a puromycin resistance cassette (puro) flanked by two *lox*P sites. A third *lox*P site was also added at a *BamH*I site 0.6 kb upstream of *Rb* exon 3 (see Fig. 1A). Presence of this 5′ *lox*P site in the genomic DNA of the ES cells after electroporation was verified by PCR using two primers surrounding this site. Details on the cloning strategy, the plasmids, and the PCR reactions are available on request. Proper integration and recombination at the *Rb* locus were confirmed by Southern blot.

Culture of MEFs

MEFs were derived from day 12.5–14.5 postcoitum embryos (Brugarolas et al. 1998) obtained by breeding or after injection of mutant ES cells into blastocysts and reimplantation into foster mothers. $Rb^{-/-}$, $p107^{-/-};p130^{-/-}$, and TKO MEFs derived from chimeric embryos were selected for two passages (5–7 d) with the appropriate antibiotics. MEFs were frozen at passage 2 or 3, and except for long-term culture, were used before passage 6. Only pure populations of MEFs were used, as assayed by genomic PCR. Genotyping was performed as described (Williams et al. 1994; Cobrinik et al. 1996; Lee et al. 1996). MEFs and the ΦNX ecotropic packaging cell line were grown in DMEM supplemented with 10% IFS (Sigma), 5mM Glutamine, and penicillin/streptomycin. All the cells were negative for mycoplasma (MycoTest kit, GIBCO BRL).

Retroviral vectors and retroviral transduction

MEFs were infected with high-titers retrovirus stocks produced by transient transfection of ΦNX cells (Serrano et al. 1997). The efficiency of infection was always >80% (data not shown). The pBabe-puro empty vector containing a constitutively active Valine 12 mutant *H-Ras* cDNA (*H-ras*V12; Serrano et al. 1997) were gifts from S. Lowe (Cold Spring Harbor Laboratory). The day before the infection, cells were plated at 10^6 (controls) or 2×10^6 (TKO) cells per 10-cm dish. Infected MEFs were selected for 3 d with 2.5 μg/mL of Puromycin (Sigma) and replated for the corresponding assays. The human *RB* cDNA (a gift from W. Kaelin, Dana Farber Institute) was subcloned in the pMIG retrovirus (obtained from H. Lodish, Whitehead Institute).

Immortalization and transformation assays

All experiments were repeated at least three times, using cells from different embryos. For growth curves, 3×10^4 cells were plated into 12-well plates and fed every other day. Serial 3T3 cultivation was conducted as described (Todaro and Green 1963). Briefly, 3×10^5 cells were plated on 6-cm plates; 3 d later, the total number of cells was counted and 3×10^5 cells were plated again. The cumulative increase in cell number was calculated according to the formula $\text{Log}(N_f/N_i)/\text{Log}2$, where N_i and N_f are the initial and final numbers of cells plated and counted after 3 d, respectively. To test for the ability of the cells to form multiple layers (foci formation assay), 10^6 MEFs from different genotypes were plated in 10-cm dishes and grown for 3 wk. The medium was changed every 3 d for the first 2 wk and then every 2 d for the final week. Plates were then stained with Giemsa (Sigma). To test for the ability of the cells to form colonies when plated at low density. 1.3×10^3 cells were plated in two 10-cm dishes and fed every 3 d. After 2 wk, dishes were stained with Giemsa and the number of visible colonies was counted. For colony formation in semisolid medium, 5.10^4 cells were plated in DMEM with 15% serum and 0.3% low–melting point agarose (LMP, GIBCO BRL) onto 6-cm dishes coated with 0.5% LMP. Cultures were fed weekly. To test for tumorigenicity, exponentially growing cells were resuspended in PBS at 10^7 cells/mL, 10^6 cells were injected subcutaneously into nude mice (Swiss *nu*/*nu*, Jackson Laboratories), and tumor development was monitored during 6 wk. MEFs infected with the pBabe-*HrasV12*-puro or the pBabe-puro retroviruses were selected for 3 d in 2.5 μg/mL puromycin, then replated to be expanded and injected into nude mice 7–8 d after infection.

Cell cycle, cell size, and cell death assays

Cells were prepared for cell cycle analysis as described (Brugarolas et al. 1998). Samples were processed using a FACScan apparatus (Becton Dickinson), and data were analyzed using the ModFit LT software (Becton Dickinson). Cell size was measured on 2n, 4n, and whole population of cells gated from a forward-side scatter height (FSC-H)/FL2-A dot plot and represented in a FSC-H histogram (Brugarolas et al. 1998).

Cell viability and apoptosis

Adherent and nonadherent cells were pooled and analyzed for viability by Trypan blue exclusion; >100 cells were counted for each point. Apoptotic cell death was measured by staining the cells with Annexin-FITC (Pharmingen) and propidium iodide (PI; Sigma) and analyzing them by two-color cytometry using a FACScan, as described (de Stanchina et al. 1998). Annexin-positive cells (PI positive or not) were counted as apoptotic.

DNA-damage experiments

Control cells were plated at 10^6 cells per 10-cm dish, and the day after, they were γ irradiated with a dose of 5 Grays (Brugarolas et al. 1995) or treated with 0.2 μg/mL of doxorubicin (Sigma; Attardi et al. 2000). After 18 h, cells were collected and processed for cell cycle analysis or RNA preparation.

Immunoblotting

Whole-cell extracts of exponentially growing cells were prepared in lysis buffer (65 mM Tris pH7, 1% NP40, 2 mM EDTA, 100 mM NaCl) containing the Complete cocktail of proteases inhibitors (Roche), and protein concentrations were determined with the BCA protein assay reagent (Pierce). Immunoblot analysis for pRB (Pharmingen, 14001A, 1 : 250), p107 (Santa Cruz, CA, C-18, 1 : 1000), and p130 (Santa Cruz, C-20, 1 : 1000) were performed as described (Mulligan et al. 1998). Immunoblot analysis of p53 (Santa Cruz, Pab240, 1 : 500), $p16^{INK4A}$ (Santa Cruz, M-156, 1 : 1000), $p21^{CIP1}$ (Santa Cruz, C-19, 1 : 1000) $p19^{ARF}$ (Novus Biological, NB 200–106, 1 : 500), and cleaved PARP (New England Biolabs, 1 : 2000) was performed with 60–100 μg of proteins run on 12.5% acrylamide gels transferred to Immobilon-P (Millipore). Secondary antibodies coupled to HRP were purchased from Jackson ImmunoResearch Laboratories and used at 1 : 5000. Detection was performed by chemiluminescence.

Electromobility shift assays

Cell extracts were prepared and E2F binding reactions were performed as described (Mulligan et al. 1998). Briefly, complexes were separated by electrophoresis on a 4% polyacrylamide (29.2 : 0.8)-5% glycerol-0.25× Tris-Borate-EDTA gel at 175V for 4 h at 4°C. The antibodies used to supershift the complexes were p130 C-20 (Santa Cruz), p107 SD-15 (a gift from N. Dyson, MGH, Charlestown, MA), pRB 21C9 (Santa Cruz), and E2F-4 (a gift from J. Lees, MIT, Cambridge, MA). p53 assays were performed as described (Tsai et al. 1998).

Northern blot analysis

Preparation of total RNA and Northern blot analysis was performed using standard methods as described (Attardi et al. 2000).

Acknowledgments

We are grateful to B. Sauer, S. Lowe, W. Kaelin, H. Lodish, J. Lees, and N. Dyson for various useful reagents. We thank A. de Vries, K. Reilly, E. Flores, and K. Tsai for helpful discussions, and A. Brunet and K. Cichowski for critical reading of the manuscript. This work has been supported by funding from Human Frontier Science Program (J.S.) and the National Cancer Institute (T.J.). T.J. is an Associate Investigator at the Howard Hughes Medical Institute.

The publication costs of this article were defrayed in part by payment of page charges. This article must therefore be hereby marked "advertisement" in accordance with 18 USC section 1734 solely to indicate this fact.

References

Assoian, R.K. and Zhu, X. 1997. Cell anchorage and the cytoskeleton as partners in growth factor dependent cell cycle progression. *Curr. Opin. Cell. Biol.* **9:** 93–98.

Attardi, L.D., Reczek, E.E., Cosmas, C., Demicco, E.G., McCurrach, M.E., Lowe, S.W., and Jacks, T. 2000. PERP, an apoptosis-associated target of p53, is a novel member of the PMP-22/gas3 family. *Genes & Dev.* **14:** 704–718.

Brown, J.P., Wei, W., and Sedivy, J.M. 1997. Bypass of senescence after disruption of p21CIP1/WAF1 gene in normal diploid human fibroblasts. *Science* **277:** 831–834.

Bruce, J.L., Hurford, R.K., Classon, M., Koh, J., and Dyson, N. 2000. Requirements for cell cycle arrest by p16INK4a. *Molecular Cell* **6:** 737–742.

Brugarolas, J., Chandrasekaran, C., Gordon, J.I., Beach, D., Jacks T., and Hannon, G.J. 1995. Radiation-induced cell cycle arrest compromised by p21 deficiency. *Nature* **377:** 552–557.

Brugarolas, J., Bronson, R.T., and Jacks, T. 1998. p21 is a critical CDK2 regulator essential for proliferation control in Rb-deficient cells. *J. Cell Biol.* **141:** 503–514.

Clarke, A.R., Maandag, E.R., van Roon, M., van der Lugt, N.M., van der Valk, M., Hooper, M.L., Berns, A., and te Riele, H. 1992. Requirement for a functional Rb-1 gene in murine development. *Nature* **359:** 328–330.

Claudio, P.P., Howard, C.M., Pacilio, C., Cinti, C., Romano, G., Minimo, C., Maraldi, N.M., Minna, J.D., Gelbert, L., Leoncini, L., et al. 2000. Mutations in the retinoblastoma-related gene RB2/p130 in lung tumors and suppression of tumor growth in vivo by retrovirus-mediated gene transfer. *Cancer Res.* **60:**372–382.

Cobrinik, D., Dowdy, S.F., Hinds, P.W., Mittnacht, S., and Weinberg, R.A. 1992. The retinoblastoma protein and the regulation of cell cycling. *Trends Biochem. Sci.* **17:** 312–315.

Cobrinik, D., Lee, M.H., Hannon, G., Mulligan, G., Bronson, R.T., Dyson, N., Harlow, E., Beach, D., Weinberg, R.A., and Jacks, T. 1996. Shared role of the pRB-related p130 and p107 proteins in limb development. *Genes & Dev.* **10:** 1633–1644.

Dannenberg, J.-H., van Rossum, A., Schuijff, L., and te Riele, H. 2000. Ablation of the Retinoblastoma gene family deregulates G_1 control causing immortalization and increased cell turnover under growth-restricting conditions. *Genes & Dev.* **14:** 3051–3064. (This issue).

Demers, G.W., Foster, S.A., Halbert, C.L., and Galloway, D.A. 1994. Growth arrest by induction of p53 in DNA damaged keratinocytes is bypassed by human papillomavirus 16 E7. *Proc. Natl. Acad. Sci.* **91:** 4382–4386.

de Stanchina, E., McCurrach, M.E., Zindy, F., Shieh, S.Y., Ferbeyre, G., Samuelson, A.V., Prives, C., Roussel, M.F., Sherr, C.J., and Lowe, S.W. 1998. E1A signaling to p53 involves the p19(ARF) tumor suppressor. *Genes & Dev.* **12:** 2434–2442.

Dulic, V., Kaufmann, W.K., Wilson, S.J., Tlsty, T.D., Lees, E., Harper, J.W., Elledge, S.J., and Reed, S.I. 1994. p53-dependent inhibition of cyclin-dependent kinase activities in human fibroblasts during radiation-induced G_1 arrest. *Cell* **76:** 1013–1023.

Dyson, N. 1998. The regulation of E2F by pRB-family proteins. *Genes & Dev.* **12:** 2245–2262.

Flint, J. and Shenk, T. 1997. Viral transactivating proteins. *Annu. Rev. Genet.* **31:** 177–212.

Goodrich, D.W. and Lee, W.H. 1993. Molecular characterization of the retinoblastoma susceptibility gene. *Biochim. Biophys. Acta* **1155:** 43–61.

Harbour, J.W. and Dean, D.C. 2000. The Rb/E2F pathway: Expanding roles and emerging paradigms. *Genes & Dev.* **14:** 2393–2409.

Harrington, E.A., Bruce, J.L., Harlow, E., and Dyson, N. 1998. pRB plays an essential role in cell cycle arrest induced by DNA damage. *Proc. Natl. Acad. Sci.* **95:** 11945–11950.

Harvey, M., Sands, A.T., Weiss, R.S., Hegi, M.E., Wiseman, R.W., Pantazis, P., Giovanella, B.C., Tainsky, M.A., Bradley, A., and Donehower, L.A. 1993. In vitro growth characteristics of embryo fibroblasts isolated from p53– deficient mice. *Oncogene* **8:** 2457–2467.

Hengst, L. and Reed, S.I. 1998. Inhibitors of the Cip/Kip family. *Curr. Top. Microbiol. Immunol.* **227:** 25–41.

Herrera, R.E., Sah, V.P., Williams, B.O., Makela, T.P., Weinberg, R.A., and Jacks, T. 1996. Altered cell cycle kinetics, gene expression, and G_1 restriction point regulation in Rb-deficient fibroblasts. *Mol. Cell. Biol.* **16:** 2402–2407.

Holley, R.W. 1975. Control of growth of mammalian cells in cell culture. *Nature* **258:** 487–490.

Hurford, R.K., Cobrinik, D., Lee, M.H., and Dyson, N. 1997. pRB and p107/p130 are required for the regulated expression of different sets of E2F responsive genes. *Genes & Dev.* **11:** 1447–1463.

Jacks, T., Fazeli, A., Schmitt, E.M., Bronson, R.T., Goodell, M.A., and Weinberg, R.A. 1992. Effects of an Rb mutation in the mouse. *Nature* **359:** 295–300.

Jiang, Z., Zacksenhaus, E., Gallie, B.L., and Phillips, R.A. 1997. The retinoblastoma gene family is differentially expressed during embryogenesis. *Oncogene* **14:** 1789–1797.

Kamijo, T., Zindy, F., Roussel, M.F., Quelle, D.E., Downing, J.R., Ashmun, R.A., Grosveld, R., and Sherr, C.J. 1997. Tumor suppression at the mouse INK4a locus mediated by the alternative reading frame product p19ARF. *Cell* **91:** 649–659.

Kastan, M.B. 1997. Genetic instability and tumorigenesis: Introduction. *Curr. Top. Microbiol. Immunol.* **221:** 1–4.

Kastan, M.B., Zhan, Q., el-Deiry, W.S., Carrier, F., Jacks, T., Walsh, V.W., Plunkett, B.S., Vogelstein, B., and Fornace, A.J. 1992. A mammalian cell cycle checkpoint pathway utilizing p53 and GADD45 is defective in ataxia-telangiectasia. *Cell* **71:** 587–597.

LeCouter, J.E., Kablar, B., Hardy, W.R., Ying, C., Megeney, L.A., May, L.L., and Rudnicki, M.A. 1998a. Strain-dependent myeloid hyperplasia, growth deficiency, and accelerated cell cycle in mice lacking the Rb-related p107 gene. *Mol. Cell. Biol.* **18:** 7455–7465.

LeCouter, J.E., Kablar, B., Whyte, P.F., Ying, C., and Rudnicki, M.A. 1998b. Strain-dependent embryonic lethality in mice lacking the retinoblastoma- related p130 gene. *Development* **125:** 4669–4679.

Lee, E.Y., Chang, C.Y., Hu, N., Wang, Y.C., Lai, C.C., Herrup, K. Lee, W.H., and Bradley, A. 1992. Mice deficient for Rb are nonviable and show defects in neurogenesis and haematopoiesis. *Nature* **359:** 288–294.

Lee, M.H., Williams, B.O., Mulligan, G., Mukai, S., Bronson, R.T., Dyson, N., Harlow, E., and Jacks, T. 1996. Targeted disruption of p107: Functional overlap between p107 and Rb. *Genes & Dev.* **10:** 1621–1632.

Maandag, E.C., van der Valk, M., Vlaar, M., Feltkamp, C., O'Brien, J., van Roon, M., van der Lugt, N., Berns, A., and te Riele, H. 1994. Developmental rescue of an embryonic-lethal mutation in the retinoblastoma gene in chimeric mice. *EMBO J.* **13:** 4260–4268.

Medema, R.H., Herrera, R.E., Lam, E., and Weinberg, R.A. 1995. Growth suppression by p16ink4 requires functional retinoblastoma protein. *Proc. Natl. Acad. Sci.* **92:** 6289–6293.

Mulligan, G. and Jacks, T. 1998. The retinoblastoma gene family: Cousins with overlapping interests. *Trends Genet.* **14:** 223–229.

Mulligan, G.J., Wong, J., and Jacks, T. 1998. p130 is dispensable in peripheral T lymphocytes: Evidence for functional compensation by p107 and pRB. *Mol. Cell. Biol.* **18:** 206–220.

Nevins, J.R. 1994. Cell cycle targets of the DNA tumor viruses. *Curr. Opin. Genet. Dev.* **4:** 130–134.

Novitch, B.G., Mulligan, G.J., Jacks, T., and Lassar, A.B. 1996.

Skeletal muscle cells lacking the retinoblastoma protein display defects in muscle gene expression and accumulate in S and G_2 phases of the cell cycle. *J. Cell Biol.* **135:** 441–456.
Pantoja, C. and Serrano, M. 1999. Murine fibroblasts lacking p21 undergo senescence and are resistant to transformation by oncogenic Ras. *Oncogene* **18:** 4974–4982.
Pardee, A.B. 1989. G_1 events and regulation of cell proliferation. *Science* **246:** 603–608.
Robanus-Maandag, E., Dekker, M., van der Valk, M., Carrozza, M.L., Jeanny, J.C., Dannenberg, J.H., Berns, A., and te Riele, H. 1998. p107 is a suppressor of retinoblastoma development in pRb-deficient mice. *Genes & Dev.* **12:** 1599–1609.
Robertson, E.J. 1997. Derivation and maintenance of embryonic stem cell cultures. *Methods Mol. Biol.* **75:** 173–184.
Ruas, M. and Peters, G. 1998. The p16INK4a/CDKN2A tumor suppressor and its relatives. *Biochim. Biophys. Acta* **1378:** F115–177.
Samuelson, A.V. and Lowe, S.W. 1997. Selective induction of p53 and chemosensitivity in RB-deficient cells by E1A mutants unable to bind the RB-related proteins. *Proc. Natl. Acad. Sci.* **94:** 12094–12099.
Savatier, P., Lapillonne, H., van Grunsven, L.A., Rudkin, B.B., and Samarut, J. 1996. Withdrawal of differentiation inhibitory activity/leukemia inhibitory factor up-regulates D-type cyclins and cyclin-dependent kinase inhibitors in mouse embryonic stem cells. *Oncogene* **12:** 309–322.
Serrano, M., Lin, A.W., McCurrach, M.E., Beach, D., and Lowe, S.W. 1997. Oncogenic ras provokes premature cell senescence associated with accumulation of p53 and p16INK4a. *Cell* **88:** 593–602.
Sherr, C.J. 1996. Cancer cell cycles. *Science* **274:** 1672–1677.
Slebos, R.J., Lee, M.H., Plunkett, B.S., Kessis, T.D., Williams, B.O., Jacks, T. Hedrick, L., Kastan, M.B., and Cho, K.R. 1994. p53-dependent G_1 arrest involves pRB-related proteins and is disrupted by the human papillomavirus 16 E7 oncoprotein. *Proc. Natl. Acad. Sci.* **91:** 5320–5324.
Smith-McCune, K., Kalman, D., Robbins, C., Shivakumar, S., Yuschenkoff, L., and Bishop, J.M. 1999. Intranuclear localization of human papillomavirus 16 E7 during transformation and preferential binding of E7 to the Rb family member p130. *Proc. Natl. Acad. Sci.* **96:** 6999–7004.
Stein, G.H. and Dulic, V. 1998. Molecular mechanisms for the senescent cell cycle arrest. *J. Investig. Dermatol. Symp. Proc.* **3:** 14–18.
Takimoto, H., Tsukuda, K., Ichimura, K., Hanafusa, H., Nakamura, A., Oda, M., Harada, M., and Shimizu, K. 1998. Genetic alterations in the retinoblastoma protein-related p107 gene in human hematologic malignancies. *Biochem. Biophys. Res. Commun.* **251:** 264–268.
Todaro, G. and Green, H. 1963. Quantitative studies of the growth of mouse embryo cells in culture and their development into established lines. *J. Cell. Biol.* **17:** 299–313.
Tsai, K.Y., Hu, Y., Macleod, K.F., Crowley, D., Yamasaki, L., and Jacks, T. 1998. Mutation of E2f-1 suppresses apoptosis and inappropriate S phase entry and extends survival of Rb-deficient mouse embryos. *Mol. Cell* **2:** 293–304.
Weinberg, R.A. 1995. The retinoblastoma protein and cell cycle control. *Cell* **81:** 323–330.
Whyte, P., Williamson, N.M., and Harlow, E. 1989. Cellular targets for transformation by the adenovirus E1A proteins. *Cell* **56:** 67–75.
Williams, B.O., Schmitt, E.M., Remington, L., Bronson, R.T., Albert, D.M., Weinberg, R.A., and Jacks, T. 1994. Extensive contribution of Rb-deficient cells to adult chimeric mice with limited histopathological consequences. *EMBO J.* **13:** 4251–4259.
Yamasaki, L., Bronson, R., Williams, B.O., Dyson, N., Harlow, E., and Jacks, T. 1998. Loss of E2F-1 reduces tumorigenesis and extends the lifespan of Rb1(+/–)mice. *Nat. Genet.* **18:** 360–364.
Zalvide, J. and DeCaprio, J.A. 1995. Role of pRb-related proteins in simian virus 40 large-T-antigen- mediated transformation. *Mol. Cell Biol.* **15:** 5800–5810.
Zhu, L., van den Heuvel, S., Helin, K., Fattaey, A., Ewen, M., Livingston, D., Dyson, N., and Harlow, E. 1993. Inhibition of cell proliferation by p107, a relative of the retinoblastoma protein. *Genes & Dev.* **7:** 1111–1125.